



Liquid Metal Condensation in the Cavity of the HIBALL Heavy Ion Fusion Reactor

L. Pong, M.L. Corradini, R.R. Peterson and G.A. Moses

January 1985

UWFDM-614

***FUSION TECHNOLOGY INSTITUTE
UNIVERSITY OF WISCONSIN
MADISON WISCONSIN***

DISCLAIMER

This report was prepared as an account of work sponsored by an agency of the United States Government. Neither the United States Government, nor any agency thereof, nor any of their employees, makes any warranty, express or implied, or assumes any legal liability or responsibility for the accuracy, completeness, or usefulness of any information, apparatus, product, or process disclosed, or represents that its use would not infringe privately owned rights. Reference herein to any specific commercial product, process, or service by trade name, trademark, manufacturer, or otherwise, does not necessarily constitute or imply its endorsement, recommendation, or favoring by the United States Government or any agency thereof. The views and opinions of authors expressed herein do not necessarily state or reflect those of the United States Government or any agency thereof.

Liquid Metal Condensation in the Cavity of the HIBALL Heavy Ion Fusion Reactor

L. Pong, M.L. Corradini, R.R. Peterson and G.A.
Moses

Fusion Technology Institute
University of Wisconsin
1500 Engineering Drive
Madison, WI 53706

<http://fti.neep.wisc.edu>

January 1985

UWFDM-614

LIQUID METAL CONDENSATION IN THE CAVITY OF THE
HIBALL HEAVY ION FUSION REACTOR

L. Pong

M.L. Corradini

R.R. Peterson

G.A. Moses

Fusion Technology Institute
1500 Johnson Drive
University of Wisconsin-Madison
Madison, Wisconsin 53706

January 1985

UWFDM-614

ABSTRACT

In the HIBALL heavy ion beam fusion reactor design, the INPORT concept is used to protect the first surface of the reactor from damage by the high energy x-rays, ion debris and fast neutrons from the exploding target. Liquid $\text{Li}_{17}\text{Pb}_{83}$ flows through porous SiC tubes and wets the outside of the tubes with a layer of $\text{Li}_{17}\text{Pb}_{83}$. This $\text{Li}_{17}\text{Pb}_{83}$ film is evaporated on each shot by the target x-rays and ion debris. The mechanisms that control the vapor pressure of the chamber are: gas radiation, $\text{Li}_{17}\text{Pb}_{83}$ evaporation from the INPORT tubes, and gas condensation back onto the INPORT tubes. From the beam stripping cross section for Bi^{2+} ions on Pb the gas pressure (evaluated at 0°C) inside the chamber must be at or below 10^{-4} torr in order for the ion beam to reach the target and ignite it. The repetition rate is therefore determined by the time required to reestablish this pressure after a shot. Calculations are presented that indicate that this time is short enough to allow a 5 Hz repetition rate for a wide range of parameters.

1. INTRODUCTION

HIBALL⁽¹⁾ (Hheavy Ion Beam and Lithium Lead) is a conceptual reactor design for heavy ion beam driven inertial confinement fusion (ICF). The reactor chamber is shown in Fig. 1, and some of the operating parameters of the reactor chamber are listed in Table 1. A persistent technical problem in the ICF field has been the protection of the first load bearing walls from high energy target debris, x-rays and neutrons. The INPORT concept⁽²⁾ (Inhibited Flow-Porous Tube) was proposed in the HIBALL design to meet this requirement and to prolong the lifetime of the reactor cavities. The INPORT unit is a woven SiC tube, acting as the first structure facing the fusion products (see Fig. 2). It is flexible, sufficiently strong, compatible with $\text{Li}_{17}\text{Pb}_{83}$, and porous enough to allow some of the liquid metal to leak out and wet the outside of the tube. The thickness of the film (~ 1 mm) is enough to absorb the x-rays and debris from the target explosion in order to reduce the heat load of the outside structure. After absorbing this energy, the liquid film is evaporated and produces a dense gas inside the reactor chamber. The amount of vaporized mass is determined by the target design and target x-ray spectrum. In order for 80% of the ion beam to be transported and hit the target, the pressure inside the cavity must be lower than 10^{-4} torr. Therefore, the repetition rate is determined by the time required to reduce the cavity pressure to this value.

The entire evaporation-condensation sequence is shown schematically in Fig. 3. After a target explosion, the x-ray energy is deposited in 10^{-4} cm of the liquid film, which is flowing down the outside of the SiC porous tubes. The temperature of the $\text{Li}_{17}\text{Pb}_{83}$ is raised above its boiling temperature and the $\text{Li}_{17}\text{Pb}_{83}$ is vaporized. The evaporated Li and Pb vapor expands into the

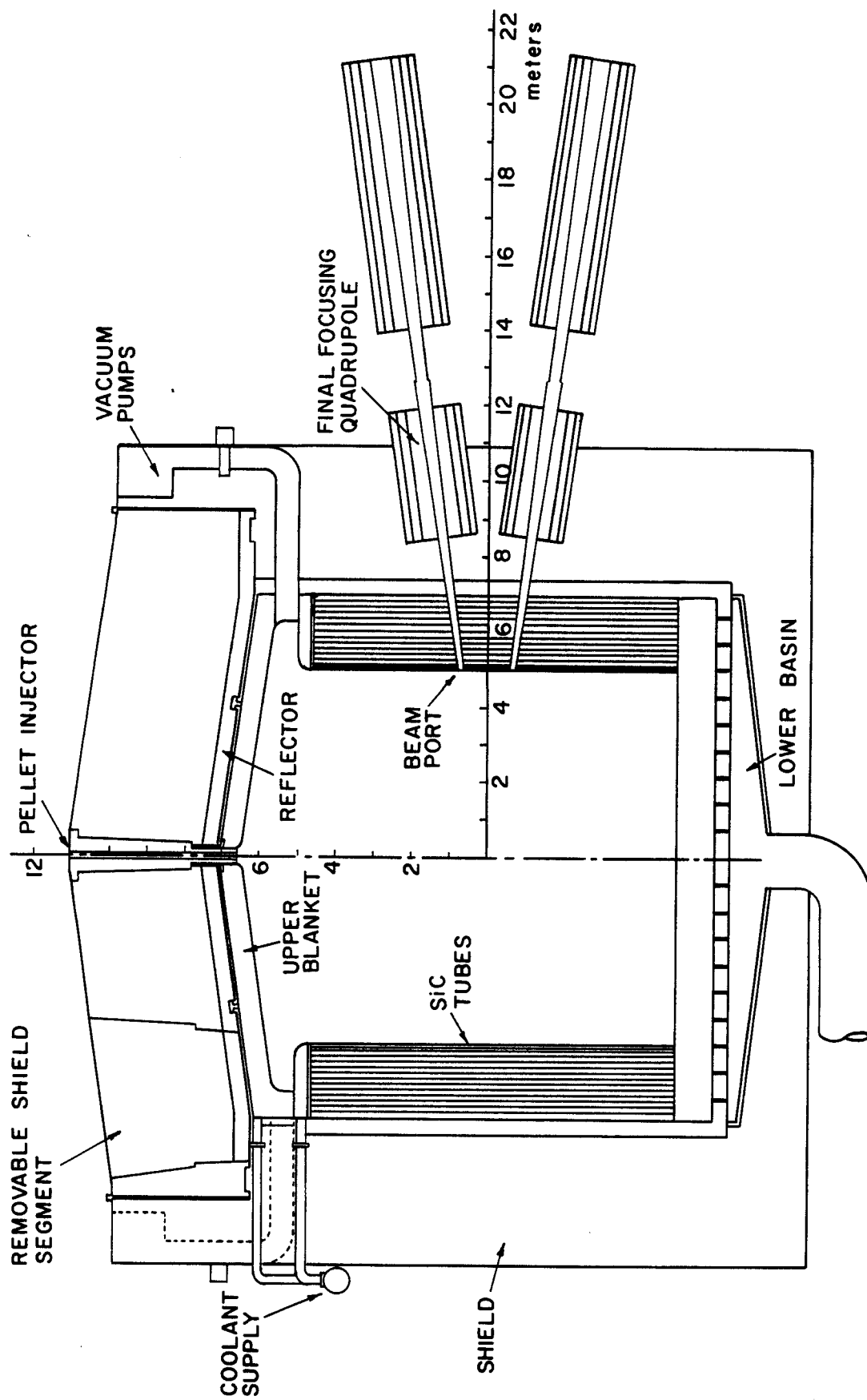


Fig. 1. Cross-sectional view of the HIBALL chamber.

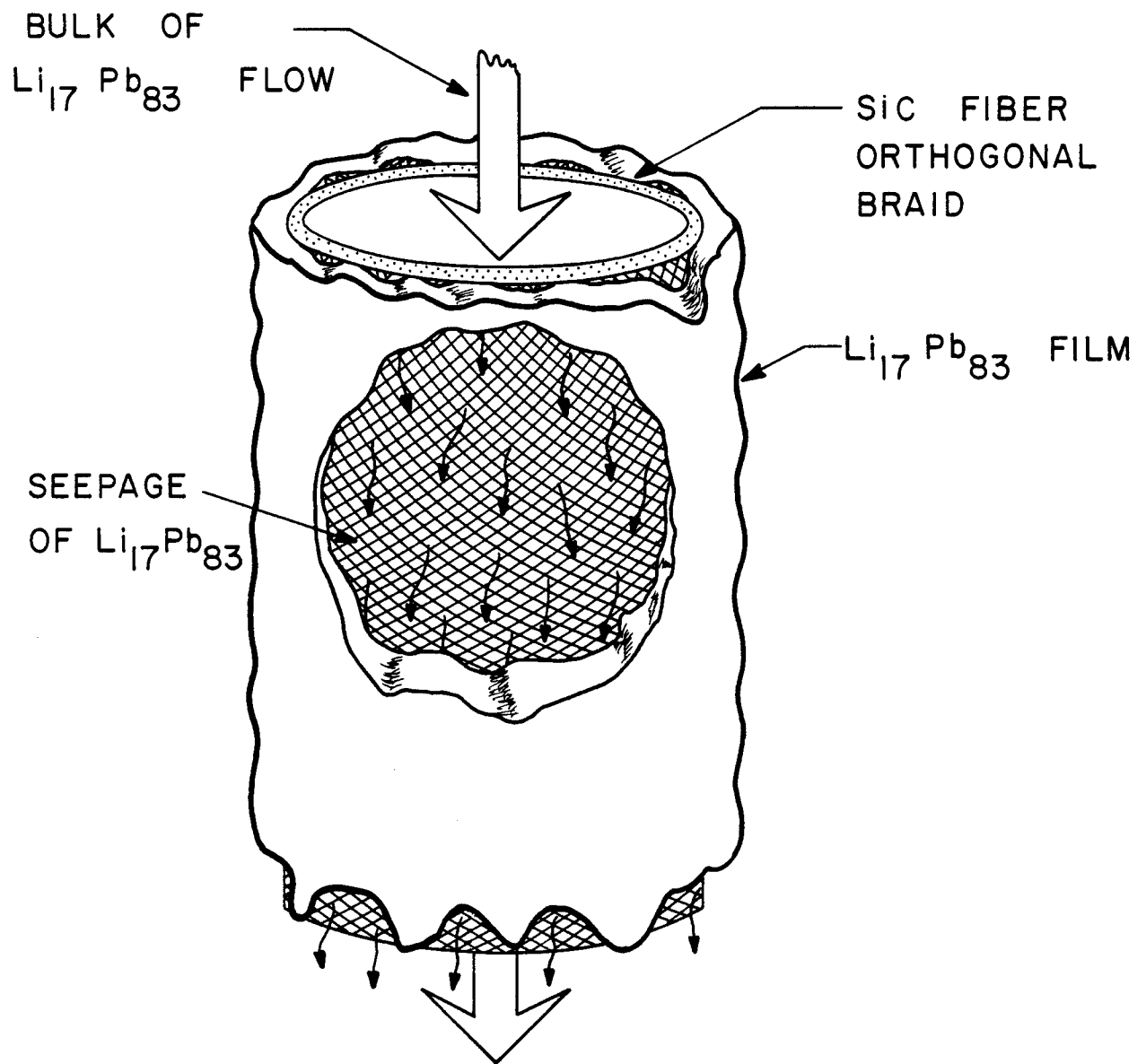


Fig. 2. Schematic of INPORT concept. Metallic coolant seeps through porous woven structure to protect outside of tube from target x-ray and ion debris.

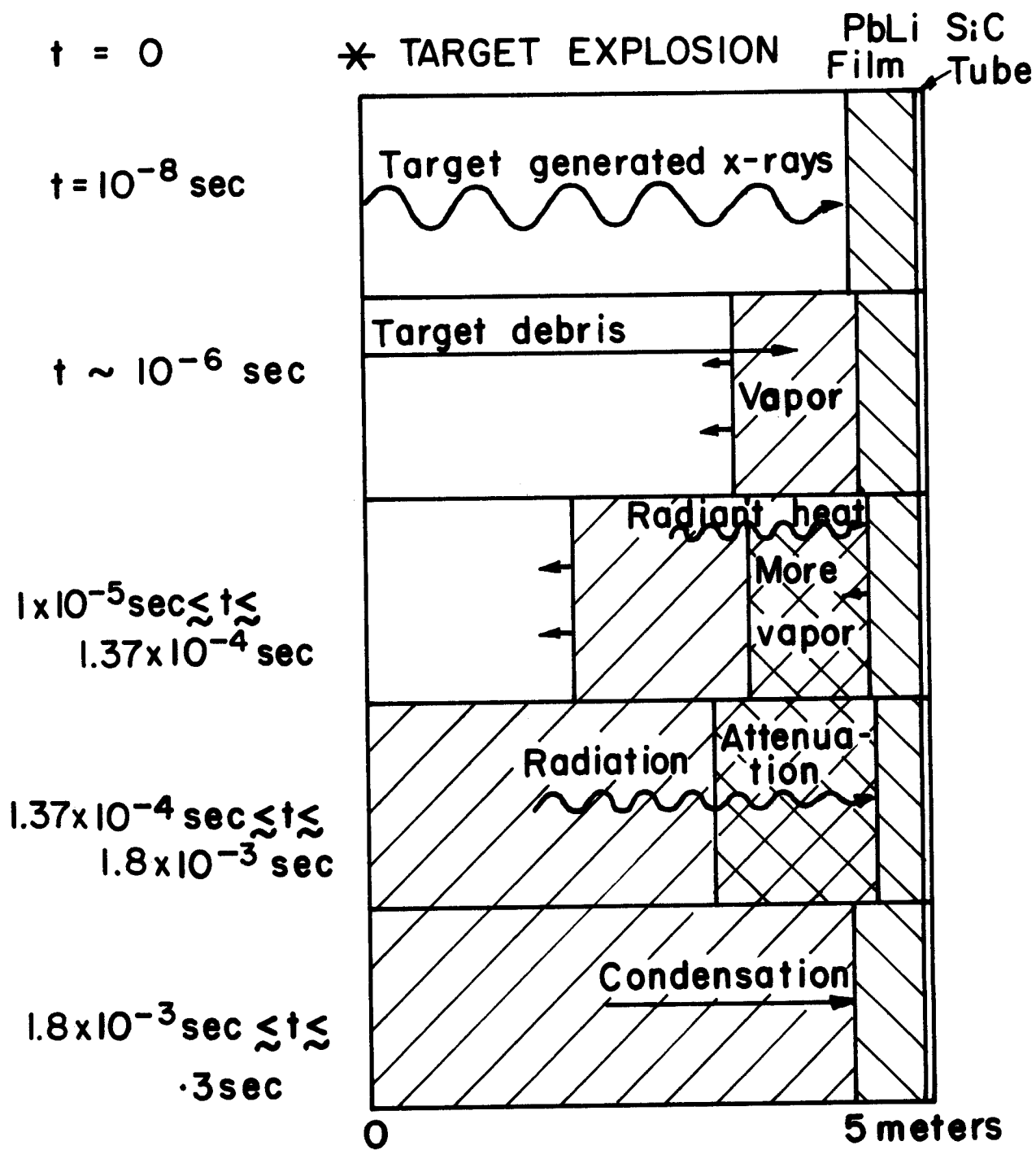


Fig. 3. History of the $\text{Li}_{17}\text{Pb}_{83}$ vapor in the HIBALL chamber.

Table 1. Selected Operating Parameters of the HIBALL Reaction Chamber

Target Yield	400 J
X-Ray and Ion Debris Energy to First Tube Bank	35 J/cm ²
INPORT Tube Length	10 m
INPORT Tube Outer Radius	
(Inner Rows)	1.5 cm
(Outer Rows)	5 cm
Amount of Li ₁₇ Pb ₈₃ Evaporated Per Shot (Nominal)	13 kg

chamber and their temperature is further raised by absorbing the energy of the ion debris. Thus the first surface is also protected from the energetic ion debris by the expanding vapor. The hot vapor then radiates energy back to the INPORT tubes, causing additional Li₁₇Pb₈₃ to be evaporated. The radiation heat flux will decrease due to the cooling of the vapor. The cooling vapor will condense back onto the surface and the energy from this condensation heat flux must be transferred into the bulk coolant flowing in the INPORT tubes. Thus, the pressure of the chamber will eventually decrease.

In this paper, we have calculated the vapor radiation, condensation and evaporation mechanisms to determine the allowable repetition rate. In Section 2 we specify the assumptions used in this analysis. The calculational procedure is explained using the base case HIBALL parameters. In Section 3 the results of the computations are presented for the base case parameters. In addition a parametric analysis is performed to show the sensitivity of the results to variations or uncertainties in two parameters, the mass of Li₁₇Pb₈₃

evaporated by the target x-rays and the thickness of film on the INPORT units. Finally in Section 4 we present our conclusions.

2. METHOD OF SOLUTION

A lumped parameter model, depicted schematically in Fig. 4, is used for this analysis. The hot vapor is allowed to radiate to the liquid metal surface and evaporate more liquid or is allowed to condense on the liquid surface, depending upon the relative magnitude of the radiative heat flux in, q_r , and the conductive heat flux out, q_{out} . The following set of assumptions are used in the calculation:

1. By neglecting the small curvature effect of the reactor chamber, a one-dimensional calculation is performed. The area and volume of the reactor chamber are conservatively calculated as $4\pi R^2$ and $4/3 \pi R^3$, where $R = 500$ cm (the radius to the first row of INPORT units).
2. The thermal physical properties of $Li_{17}Pb_{83}$ are independent of temperature and are given in Table 2 based on the recent ISPRA results.⁽³⁾
3. The calculation begins immediately after the liquid $Li_{17}Pb_{83}$ is ablated from the surface by absorption of the target x-rays.
4. The radiative processes follow the classical Stefan-Boltzmann law.
5. The mixture of Li and Pb vapor is uniformly distributed in the chamber.
6. The heat transfer coefficient between the tube wall and coolant is $4.8 \text{ W/cm}^2\text{°K}$ which is taken from $Nu = hd/k = 5 + 0.025(Re_d Pr)^{0.8}$,⁽⁴⁾ where d is the diameter of the first row INPORT tubes.
7. The equation of state for $Li_{17}Pb_{83}$ vapor⁽⁵⁾ is given in Fig. 5.

Table 2. Properties of $\text{Li}_{17}\text{Pb}_{83}$

k (W/cm $^{\circ}$ K)	0.245
μ (g/cm-s)	0.0137
P (g/cm 3)	9.43
α (cm 2 /s)	0.14949
C_p (J/g $^{\circ}$ K)	0.1738
ΔH_v (J/g)	990.99
P_{sat} (torr)	$0.83 \exp(17.86 - \frac{22300}{T}) + 0.005 \exp(18.4 - \frac{18750}{T})$
M (g/mole)	173.58

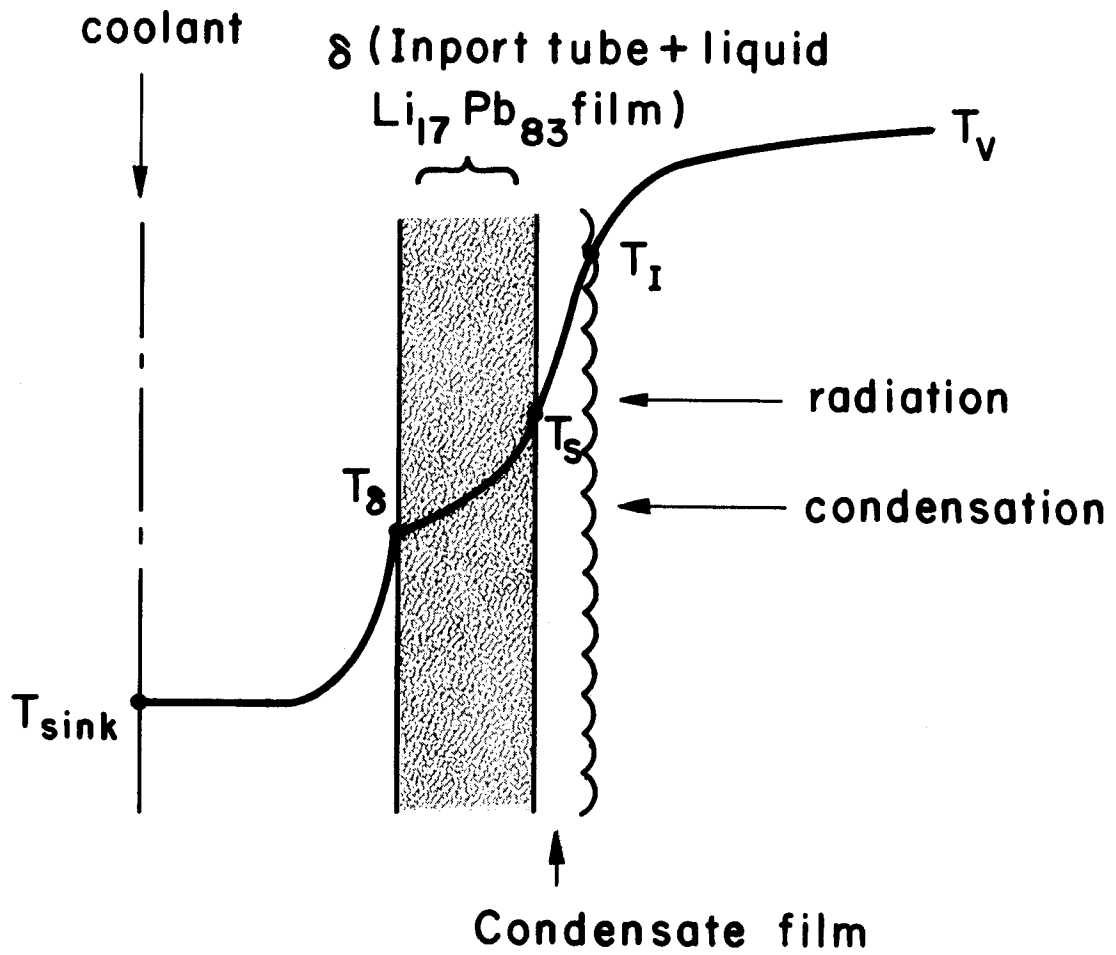


Fig. 4. Temperature profile in INPORT tube and the condensate film.

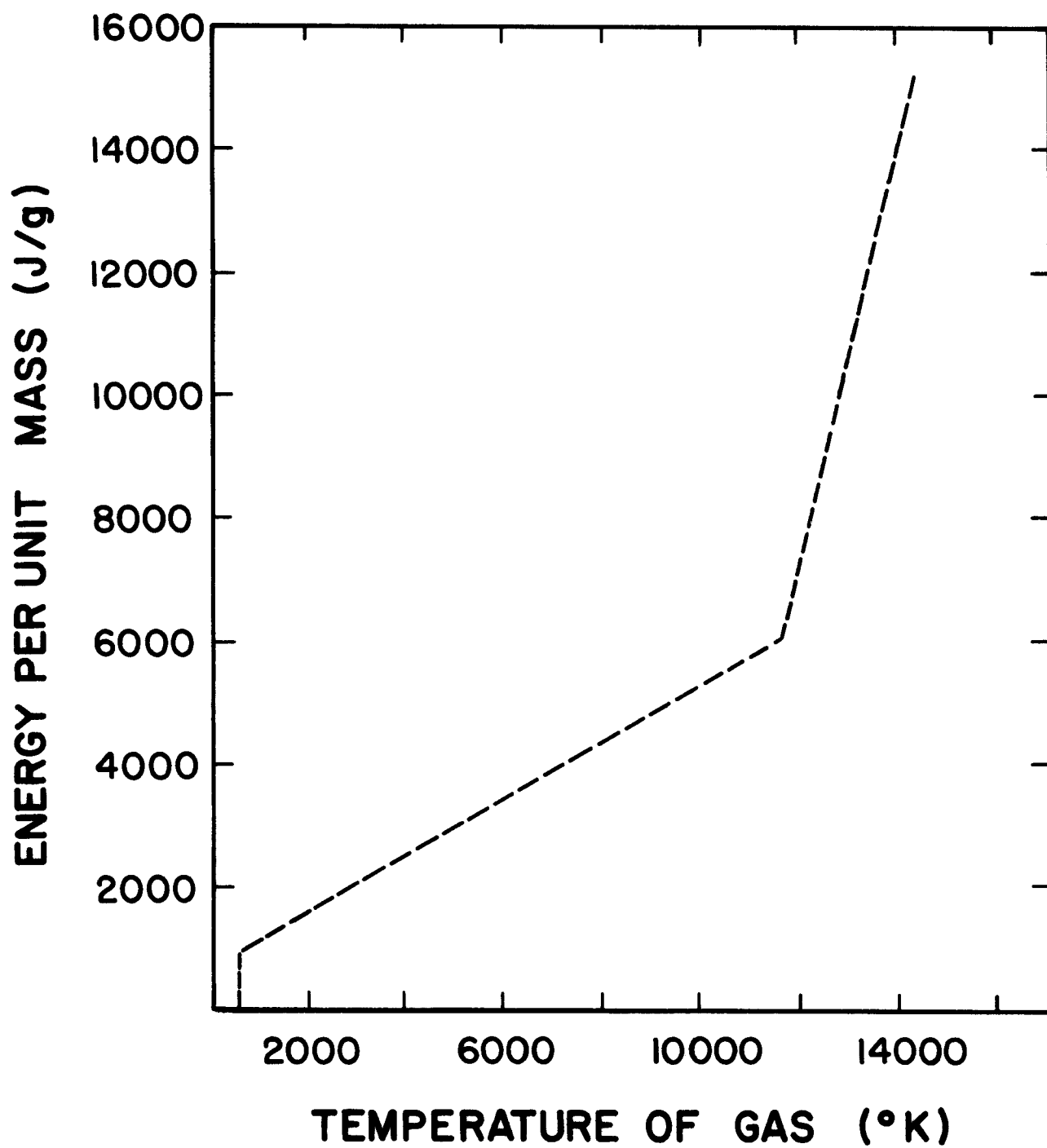


Fig. 5. The equation of state for $\text{Li}_{17}\text{Pb}_{83}$ vapor.

The procedure for calculating the time history of the evaporation condensation in the reactor cavity is outlined below for the base case HIBALL parameters.

1. Initial Conditions. After absorbing 109 MJ of energy in the form of x-rays and ion debris, the chamber conditions are:

$$E_V = 109 \text{ MJ},$$

$$T_V = 1.06 \text{ eV},$$

$$m_V = 13000 \text{ g},$$

$$P_V = 109.4 \text{ torr},$$

$$T_S = 1708^\circ\text{K},$$

$$T_{\text{sink}} = 650.5^\circ\text{K},$$

where: E_V = total energy of vapor,

T_V = temperature of vapor,

m_V = mass of vapor,

P_V = real pressure of vapor,

T_S = surface temperature of $\text{Li}_{17}\text{Pb}_{83}$ film,

T_{sink} = bulk coolant temperature.

2. Radiation. The radiation heat flux to the surface is calculated from the Stefan-Boltzmann equation:

$$q_r = \sigma(T_V^4 - T_I^4),$$

where: σ = Stefan-Boltzmann constant,

T_I = temperature of the liquid-vapor interface.

3. Evaporation. The characteristic time τ for a conduction wave to propagate through the $\text{Li}_{17}\text{Pb}_{83}$ film is:

$$\tau \sim \frac{\delta^2}{\alpha} = \frac{0.15^2}{0.1495} = 0.15 \text{ s}$$

where δ is the thickness of the film and α is the thermal diffusivity. Since τ is long (compared with the calculated result that the evaporation interval is about 10^{-4} s), it is reasonable to simplify the heat transfer of the liquid film into the following problem: a semi-infinite slab is initially at temperature T_{sink} . At time $t = 0$, the surface at $x = 0$ is suddenly raised to temperature T_{sat} and maintained at that temperature for $t > 0$, so the time dependent temperature profile and the heat flux which can be transferred into the film at $x = 0$ are:

$$T(x,t) = T_{\text{sink}} + (T_{\text{sat}} - T_{\text{sink}}) \left(1 - \operatorname{erf} \frac{x}{\sqrt{4\alpha t}}\right),$$

$$q_{\text{out}} = \frac{k}{\sqrt{\pi\alpha t}} (T_{\text{sat}} - T_{\text{sink}}),$$

where T_{sat} is the saturation temperature corresponding to the vapor pressure P_v . If the radiation heat flux, q_r , to the surface is greater than q_{out} , vaporization occurs. The conservation equations for the system are:

$$\dot{E}_v = -q_r A + \dot{m}_{\text{evap}} (\Delta H_v + C_p (T_{\text{sat}} - T_{\text{sink}})),$$

$$\dot{E}_{\text{film}} = q_{\text{out}} A,$$

$$\dot{E}_r + \dot{E}_{\text{film}} = 0,$$

$$\dot{m}_{\text{evap}} = \frac{(q_r - q_{\text{out}})A}{\Delta H_v + C_p(T_{\text{sat}} - T_{\text{sink}})} ,$$

where: \dot{E}_v = energy transfer rate of the vapor,
 \dot{E}_{film} = energy transfer rate of the film,
 ΔH_v = latent heat of vaporization for $\text{Li}_{17}\text{Pb}_{83}$,
 C_p = specific heat of $\text{Li}_{17}\text{Pb}_{83}$,
 \dot{m}_{evap} = evaporation rate.

When q_r is less than q_{out} , evaporation ceases and condensation begins.

4. Condensation. If the bulk pressure of Li or Pb is greater than the saturation pressure corresponding to the surface temperature T_I , condensation will occur. For HIBALL operating conditions, a small amount of noncondensable D_2 , T_2 , and He gas will be present and will retard the vapor condensation. The pressure⁽¹⁾ of D_2 , T_2 and He evaluated at 400°C is

$$P_{\text{D,T}} (\text{torr}) = 1.94 \times 10^{-4} \exp(-2.483 t) ,$$

$$P_{\text{He}} (\text{torr}) = 1.55 \times 10^{-4} \exp(-1.662 t) .$$

In this calculation, the noncondensable D_2 , T_2 and He gas are grouped into an effective gas with pressure P_{gas} and molecular weight M_{gas} :

$$P_{\text{gas}} = P_{\text{D,T}} + P_{\text{He}} ,$$

$$M_{\text{gas}} = \frac{M_{\text{D,T}} P_{\text{D,T}} + M_{\text{He}} P_{\text{He}}}{P_{\text{gas}}} .$$

The condensation of Li and Pb vapor is controlled by the interface resistance of the liquid-vapor and gas mixture and the resistance of the condensate film (see Fig. 4). The heat flux which can be transferred through the Nusselt film Q_{NU} is:

$$q_{NU} = h_f(T_I - T_s) ,$$

where $h_f = 17.5 \text{ W/cm}^2\text{°K}$ which is taken as the average turbulent heat transfer coefficient from the Colburn equation:⁽⁷⁾

$$\frac{h_f}{k} \left[\frac{\mu^2}{\rho^2 g} \right]^{1/3} = 0.056 \text{ Re}^{0.2} \left(\frac{C_p \mu}{k} \right)^{1/3} ,$$

where the Reynold's number $\text{Re} = 4\Gamma/\mu$, and Γ is the flow rate per unit width at the axial location $z = 500 \text{ cm}$. The condensation rate j accounting for the presence of noncondensable gas is calculated from the following equation:⁽⁸⁾

$$j = \frac{1.67}{(2\pi R_v T_v)^{1/2}} (p_v - 0.579 p_{\text{gas}} \frac{M_{\text{gas}}}{M_v} - p_I) (1 + 0.515 \ln \frac{p_v}{p_I} (\frac{T_I}{T_v})^{1/2}) \\ * (1 + 4.3 (\frac{p_{\text{gas}}}{p_I})^{0.52} (\frac{M_{\text{gas}}}{M_v})^{0.74} (\frac{T_I}{T_v})^{4.712})^{-1} ,$$

where R_v is the gas constant of the vapor, and p_I is the saturation pressure corresponding to T_I .

The governing equations for the system are:

$$q_{\text{cond}} = j_{\text{Pb}} \Delta H_{\text{Pb}} + j_{\text{Li}} \Delta H_{\text{Li}} ,$$

$$q_r = \sigma(T_v^4 - T_I^4) ,$$

$$q_{tot} = q_{cond} + q_r ,$$

$$q_{NU} = h_f(T_I - T_s) = q_{tot} ,$$

$$\dot{m}_{cond} = (j_{Li} + j_{pb})A ,$$

$$\dot{E}_v = -q_{tot} A ,$$

$$\dot{E}_{film} = q_{NU} A ,$$

$$\dot{E}_v + \dot{E}_{film} = 0 ,$$

and

$$\frac{\partial^2 T}{\partial x^2} = \frac{1}{\alpha} \frac{\partial T}{\partial x}$$

with the boundary conditions:

$$-k \left. \frac{\partial T}{\partial x} \right|_{x=0} = q_{tot} ,$$

$$-k \left. \frac{\partial T}{\partial x} \right|_{x=\delta} = h(T_\delta - T_{sink}) ,$$

where: q_{cond} = condensation heat flux,

\dot{m}_{cond} = condensation rate,

$h = 4.8 \text{ W/cm}^2\text{°K}$ based on assumption 6.

3. RESULTS

For 13 kg initial evaporated mass after the x-ray deposition, the calculation results are shown in Figs. 6-11. The surface heating due to radiation, condensation and conduction is shown in Fig. 6. At times less than 1.37×10^{-4} s, q_r is greater than q_{out} . This excess energy is used to vaporize additional $Li_{17}Pb_{83}$. After 1.5×10^{-2} s, the vapor radiation is insignificant compared to the condensation. Figure 7 shows the evaporation and condensation rates. The time lag between evaporation and condensation occurs because during this time interval the vapor pressure of Li and Pb is smaller than the saturation pressure $P_{sat}(Li)$ and $P_{sat}(Pb)$ of the interface, so no condensation occurs. After 1.8×10^{-3} s, the surface temperature will decrease further due to conduction, then Li and Pb vapor will begin to condense together. The temperature variations of the vapor-liquid interface, film surface and film-coolant interface versus time are shown in Fig. 8. The abrupt jump of the interface temperature T_I is due to the start of condensation. The temperature difference $T_I - T_s$ is large in the beginning and approaches zero at the end. This reveals that in the early stage of condensation, the condensate film controls, while in the late stage, the resistance of the bulk mixture controls the condensation process. The film-coolant interface temperature T_s does not change until 10^{-2} s which justifies the constant background temperature T_{sink} ($= 650.5^\circ K$) assumption in the evaporation part. Figure 9 shows the vapor temperature profile. The decrease of vapor temperature is governed by radiation and condensation processes. Before the time 1.8×10^{-3} s, the rapid decrease of the vapor temperature is from the radiative cooling. At 1.8×10^{-3} s, condensation begins. Since the condensation process now is controlled by the condensate film, the high interface temperature T_I will cause a smaller

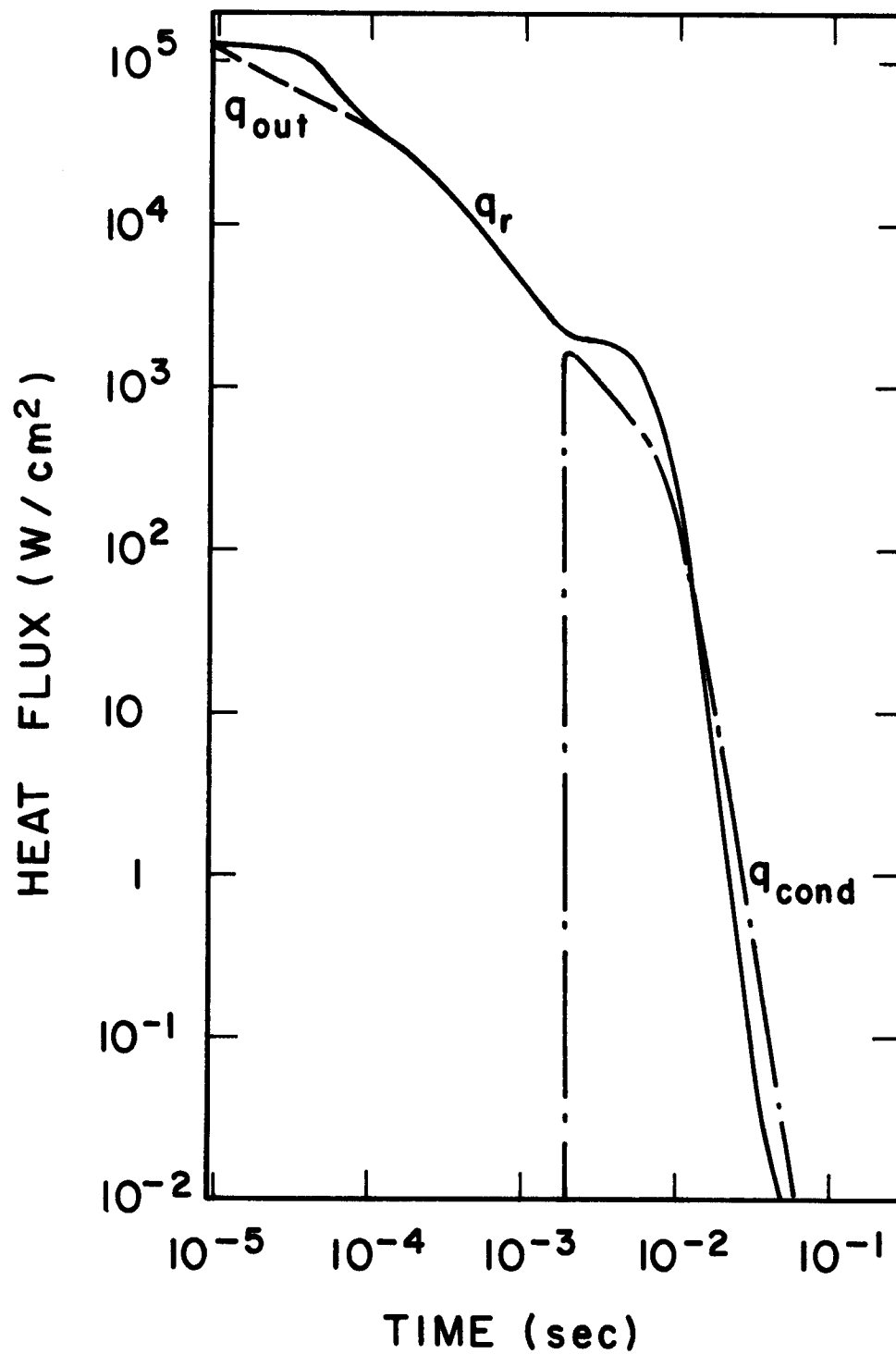


Fig. 6. First surface heat flux from radiation, condensate and conduction.

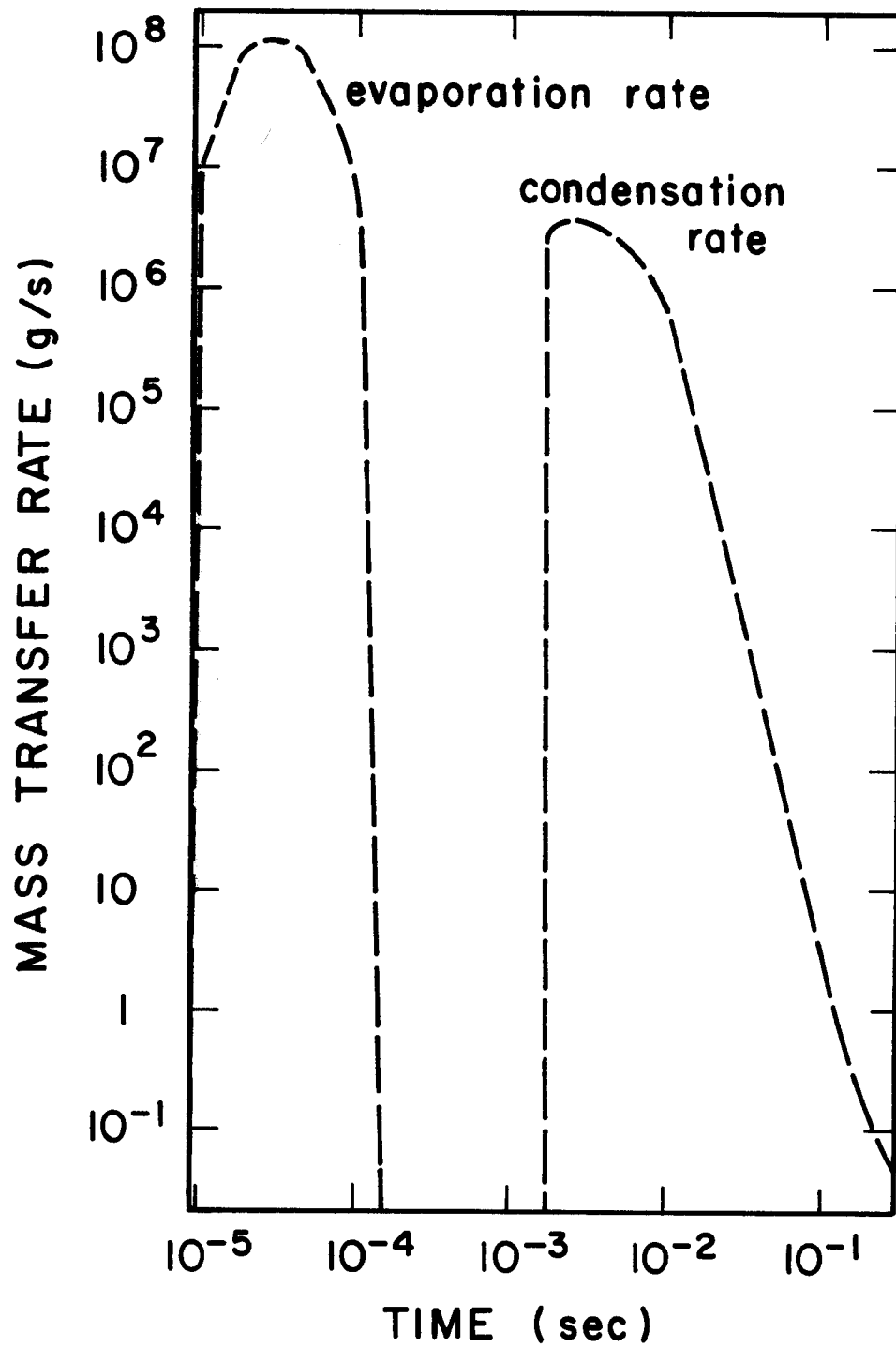


Fig. 7. Evaporation and condensation rates on first surface for mass of vaporized gas = 13 kg.

temperature vs. time

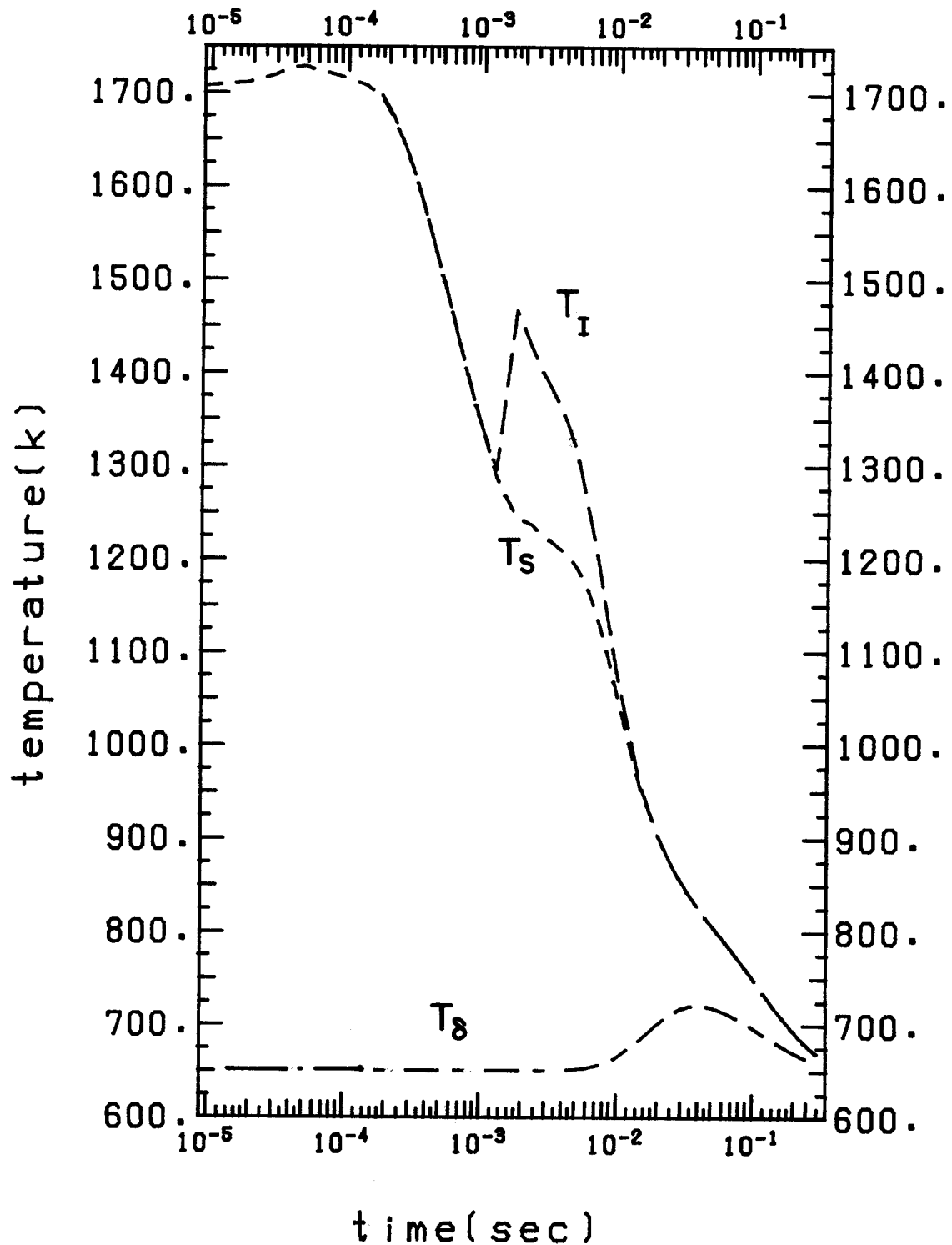


Fig. 8. Temperature of the vapor-liquid interface, film surface, and film-coolant interface versus time.

vapor temperature vs. time

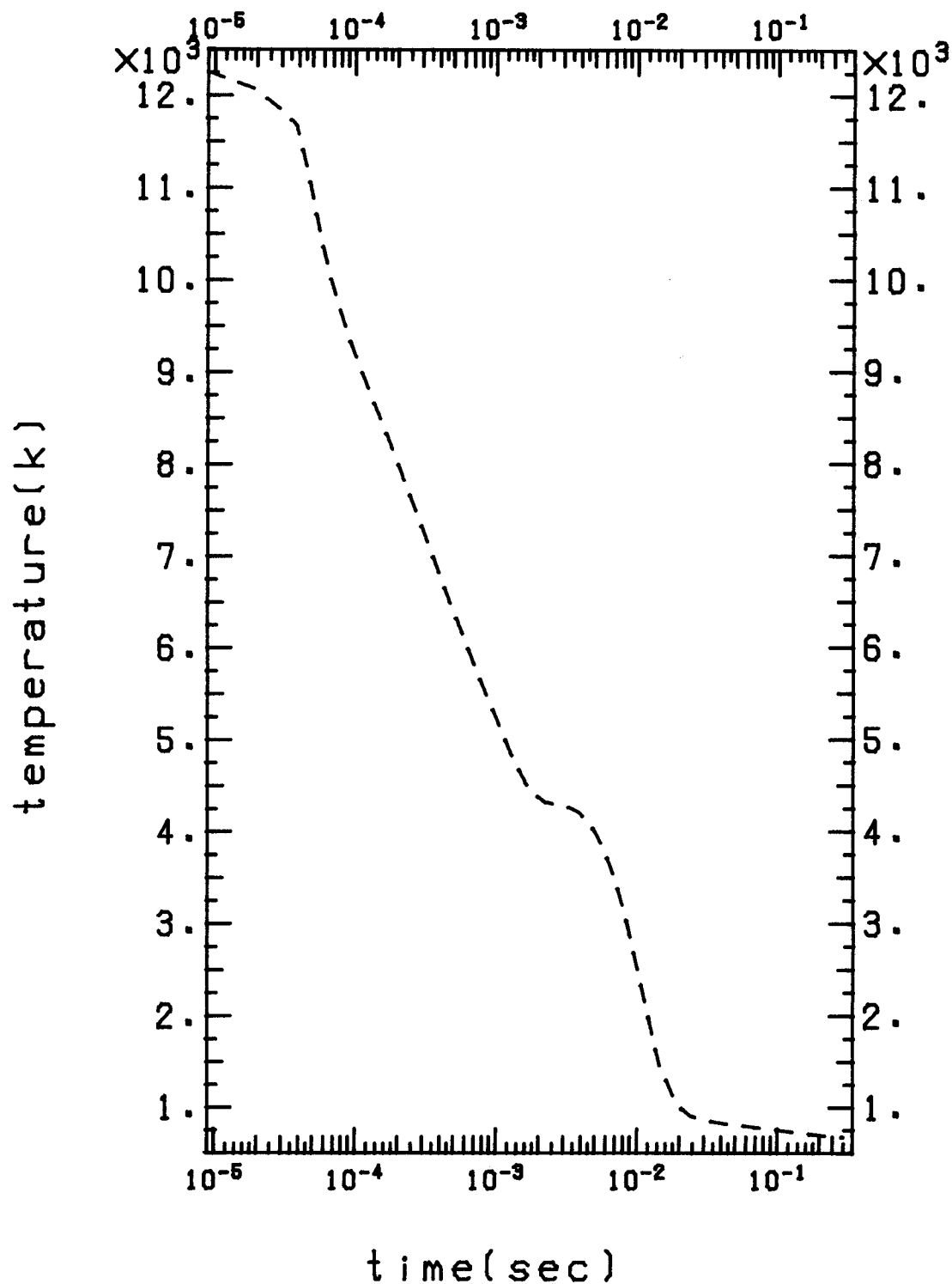


Fig. 9. $\text{Li}_{17}\text{Pb}_{83}$ vapor temperature as a function of time.

pressure vs. time

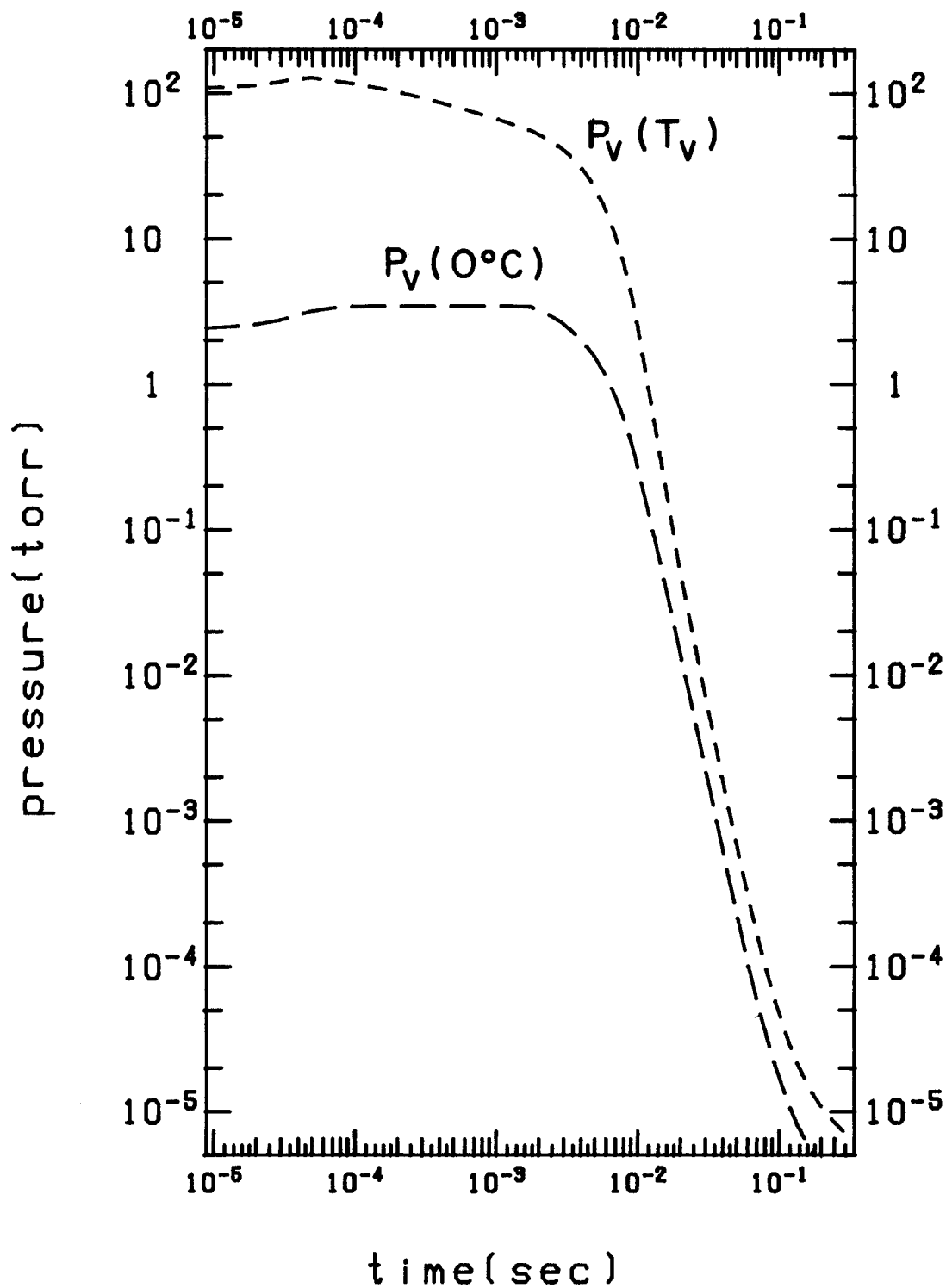


Fig. 10. Cavity pressure versus time.

mean free path vs. time

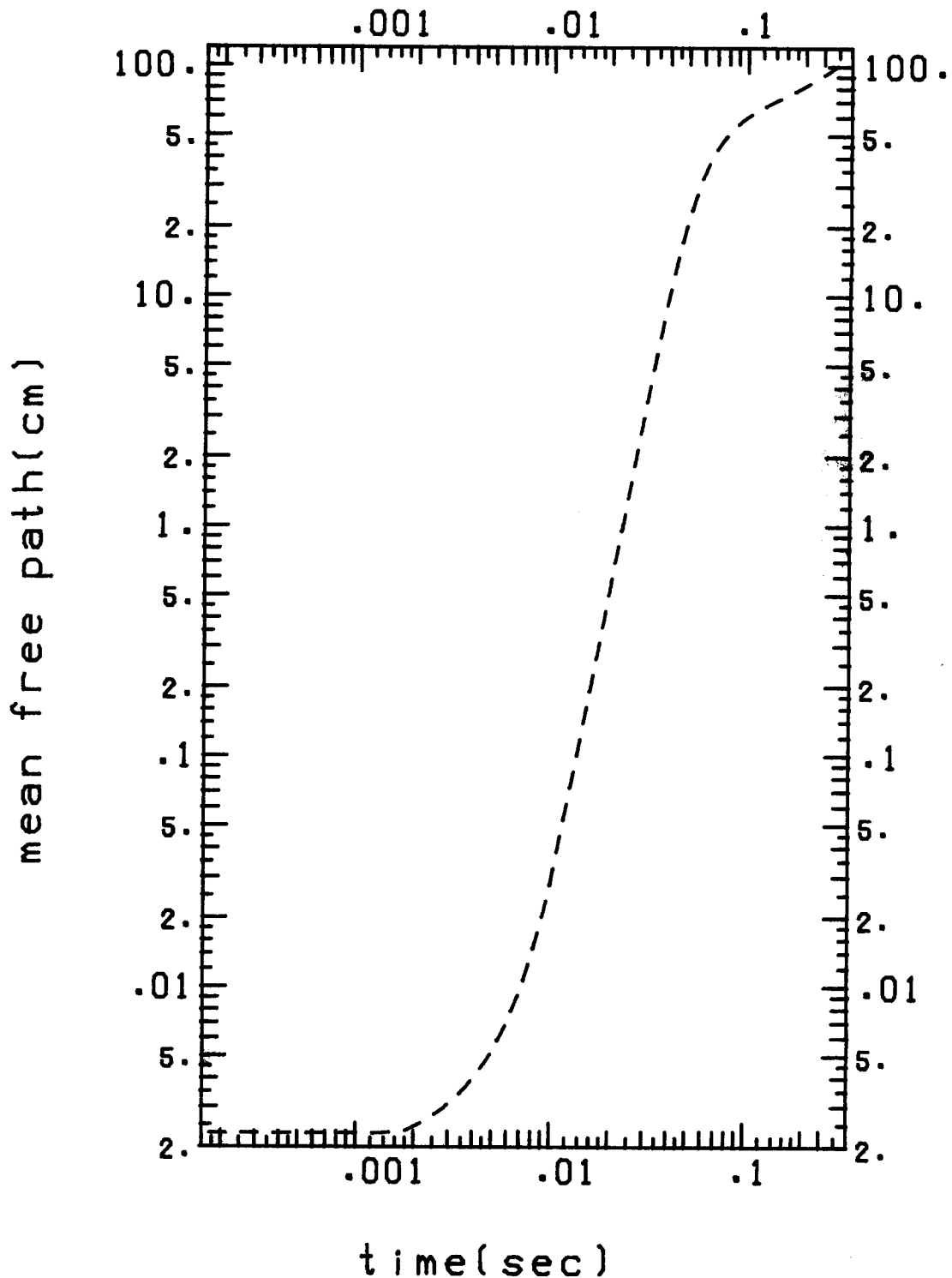


Fig. 11. The variation of mean free path in HIBALL chamber with time.

energy transfer rate from vapor to surface, so the vapor temperature will not drop as quickly as before. Later the condensate film will be able to transfer all the energy from vapor condensation, and the cooling rate of vapor will grow large again. Eventually the vapor temperature will approach the surface temperature. Figure 10 shows the real pressure ($= n_v k T_v$) and the pressure evaluated at 0°C as functions of time. The pressure P_v (0°C) will fall below 10^{-4} torr after 0.065 s. The mean free path sketch of Fig. 11 shows that up to 0.2 s, the mean free path of the mixture is still small compared to the HIBALL chamber size. This indicates that the flow is in the continuous flow regime rather than in the molecular flow regime and verifies that the lumped parameter model is applicable in this calculation. From these results, the whole process, divided into 7 stages and shown in Fig. 3, can be quantitatively summarized as follows:

1. Target explosion.
2. 13 kg of film is vaporized by the target x-rays.
3. The vapor begins expanding toward the center of the chamber and absorbs the energy of the ion debris. After about 9×10^{-6} s, the vapor temperature is raised to about 1.06 eV.
4. The vapor begins radiating energy onto the INPORT tubes.
5. An additional 5.48 kg of $\text{Li}_{17}\text{Pb}_{83}$ is evaporated from the tubes by this radiation heat flux.
6. Evaporation stops and the cooling gas begins to condense back onto the tubes at 1.8×10^{-3} s.
7. After about 0.065 s, the vapor pressure P_v (0°C) falls below 10^{-4} torr, the value required for beam propagation without excessive stripping.

This implies that a repetition rate of 15 Hz could be supported by the HIBALL cavity. This value is a factor of three larger than the 5 Hz that was chosen for the conceptual design.

These detailed results have been given for a specific case, the HIBALL base case parameters. To test the sensitivity of the results to variations or uncertainties in the target spectrum and the INPORT unit design, the initial vaporized mass and the film thickness were varied around their base case values. For 13 kg vaporized mass, the calculated vapor pressure P_v (0°C) at 0.065 s for the film thicknesses 0.1, 0.15 and 0.2 cm are 9.29×10^{-5} , 8.75×10^{-5} and 8.66×10^{-5} torr, respectively. It is concluded that the uncertainty coming from the INPORT film thickness design can be neglected. For 0.15 cm film thickness, the results for the initial vaporized mass of 6.5 kg, 13 kg and 26 kg are plotted in Figs. 12 and 13. Figure 12 shows the condensation and evaporation rates. No further evaporation occurs for the 26 kg mass. Figure 13 shows the vapor pressure P_v (0°C) versus time. The pressure of the 6.5 kg case is the lowest in the beginning, then strong evaporation increases the pressure to approximately the vapor pressure of 13 kg mass. At the end, the pressure curves of all three different initial masses converge to a single curve. From this we conclude that the chamber evacuation is insensitive to the variation of the initial vaporized mass.

4. CONCLUSIONS AND COMMENTS

The area (314 m^2) used in the calculation for vapor condensation is the projected area of the INPORT tubes. The total surface area including the backside of the first front row of INPORT tubes is 1160 m^2 , 3.6 times larger than the projected area. The vapor will actually condense faster than the

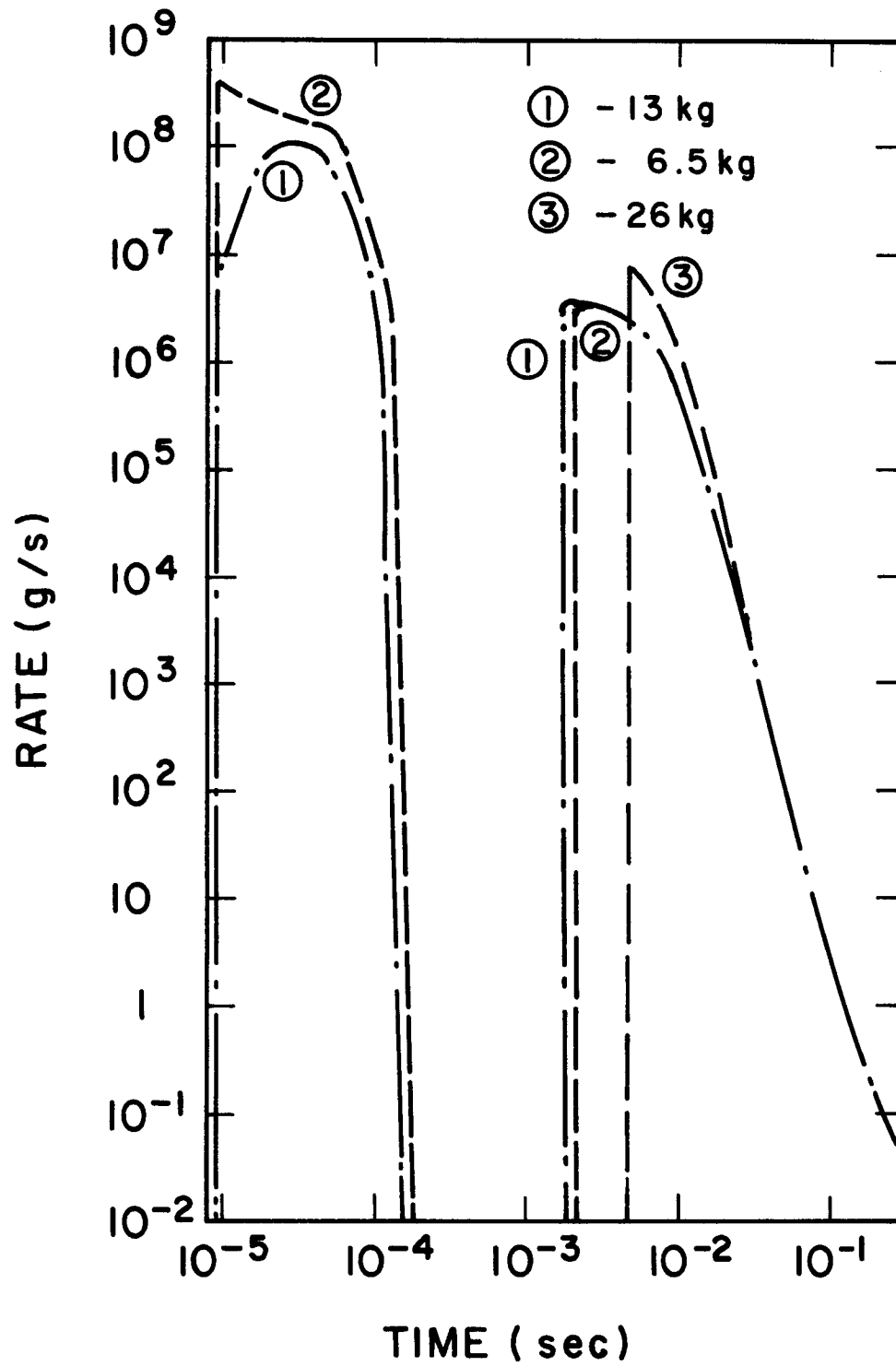


Fig. 12. Condensation and evaporation rates for 6.5 kg, 13 kg and 26 kg initial vaporized mass.

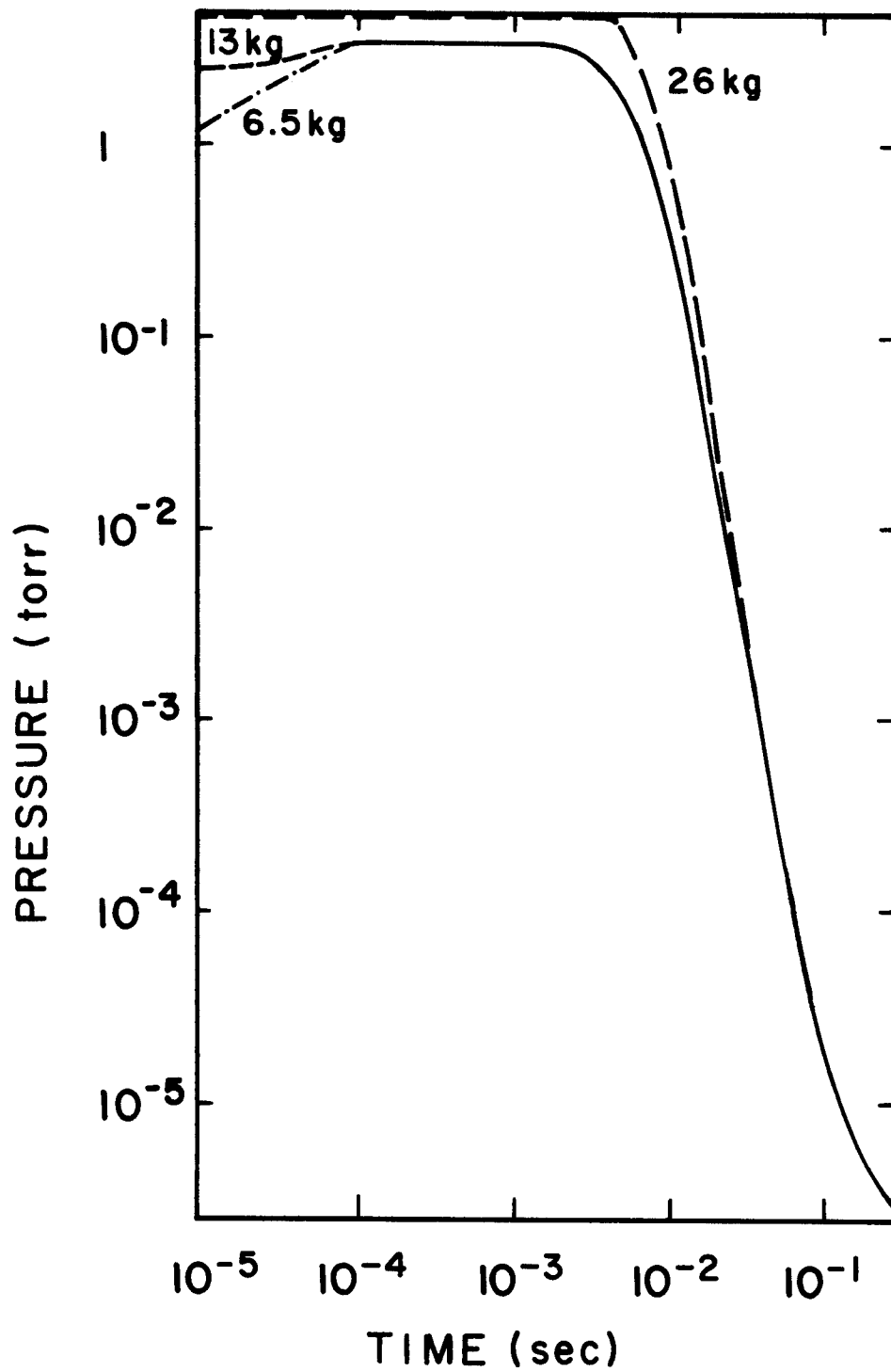


Fig. 13. Cavity pressure P_v (0°C) versus time for 6.5 kg, 13 kg and 26 kg initial vaporized mass.

predictions of these calculations since the actual area present for vapor recondensation is likely to be larger than the projected area. Our calculation is conservative from this point of view.

In summary, the vaporization, radiation and condensation phenomena of $\text{Li}_{17}\text{Pb}_{83}$ from the film of the INPORT tubes in the HIBALL conceptual reactor design have been considered. The initial mass of the $\text{Li}_{17}\text{Pb}_{83}$ vaporized by the target generated x-rays is 13 kg and the calculated result shows that the 5 Hz repetition rate of HIBALL is consistent with the chamber evacuation to 10^{-4} torr for beam propagation.

ACKNOWLEDGEMENT

This work was supported in part by Kernforschungszentrum Karlsruhe.

REFERENCES

1. B. Badger et al., "HIBALL - A Conceptual Heavy Ion Beam Driven Fusion Reactor Study," University of Wisconsin Fusion Technology Institute Report UWFD-450 (December 1981).
2. G.L. Kulcinski et al., "The INPORT Concept - An Improved Method to Protect ICF Reactor First Walls," University of Wisconsin Fusion Technology Institute Report UWFD-426 (August 1981).
3. V. Coen, "Lithium Lead Eutectic as Breeding Material in Fusion Reactors," the First International Conference on Fusion Reactor Materials, Tokyo, Japan (December 1984).
4. J.P. Holman, Heat Transfer, (1972), Chapter 6.
5. R.R. Peterson, private communication.
6. R.B. Bird, W.E. Stewart and E.N. Lightfoot, Transport Phenomena, John Wiley & Sons (1960), Chap. 11.
7. J.G. Collier, Convective Boiling and Condensation, Second Edition, McGraw-Hill (1972), Chapter 10.
8. L. Pong and G.A. Moses, "Vapor Condensation in the Presence of a Noncondensable Gas," University of Wisconsin Fusion Technology Institute Report UWFD-565, also submitted to the International Journal of Heat and Mass Transfer (January 1985).

Figure Captions

- Fig. 1. Cross-sectional view of the HIBALL chamber.
- Fig. 2. Schematic of INPORT concept. Metallic coolant seeps through porous woven structure to protect outside of tube from target x-ray and ion debris.
- Fig. 3. History of the $\text{Li}_{17}\text{Pb}_{83}$ vapor in the HIBALL chamber.
- Fig. 4. Temperature profile in INPORT tube and the condensate film.
- Fig. 5. Specific energy of $\text{Li}_{17}\text{Pb}_{83}$ as a function of temperature.
- Fig. 6. First surface heat flux from radiation, condensation and conduction.
- Fig. 7. Evaporation and condensation rates on first surface for mass of vaporized gas = 13 kg.
- Fig. 8. Temperature of the vapor-liquid interface, film surface, and film-coolant interface versus time.
- Fig. 9. $\text{Li}_{17}\text{Pb}_{83}$ vapor temperature as a function of time.
- Fig. 10. Cavity pressure versus time.
- Fig. 11. The variation of mean free path in HIBALL chamber with time.
- Fig. 12. Condensation and evaporation rates for 6.5 kg, 13 kg and 26 kg initial vaporized mass.
- Fig. 13. Cavity pressure P_v ($^{\circ}\text{C}$) versus time for 6.5 kg, 13 kg and 26 kg initial vaporized mass.